Journal of Energy Storage 52 (2022) 104761

Contents lists available at ScienceDirect

Journal of Energy Storage

journal homepage: www.elsevier.com/locate/est

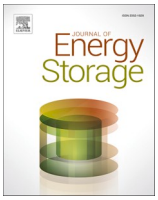

Research papers

State of charge estimation for a group of lithium-ion batteries using long short-term memory neural network

Eyad Almaita [a], Saleh Alshkoor [b], Emad Abdelsalam [c], Fares Almomani [d,*]

[a] Department of Power and Mechatronics Engineering, Tafila Technical University, Tafila, Jordan
[b] Technical Control Department, Energy and Mineral Regulatory Commission (EMRC), Jordan
[c] School of Engineering Technology, Al Hussein Technical University, Amman 11831, Jordan
[d] Department of Chemical Engineering, College of Engineering, Qatar University, Doha, Qatar

ARTICLE INFO

Keywords:
State of charge
Battery service life
Lithium-ion batteries
Machine learning
Smart energy

ABSTRACT

The present paper estimates for the first time the State of Charge (SoC) of a high capacity grid-scale lithium-ion battery storage system used to improve the power profile in a distribution network. The proposed long short-term memory (LSTM) neural network model can overcome the problems associated with the nonlinear battery model and adapt to the complexity and uncertainty of the estimation process. The accuracy of the developed model was compared with results obtained from Feed-Forward Neural Network (FFNN) topology and Deep-Feed-Forward Neural Network (DFFNN) topology under three different time series. The system was trained using real data from the Al-Manara PV power plant. The LSTM with learn-and-adapt-to-train-date properties, as well as the idea of "forget gate," shows exceptional ability to determine the SoC under various ID data. The LSTM properly calculated the SoC for all three-time models with a maximum standard error (MSE) of less than 0.62%, while the FFNN and DFFNN provided a fair estimate for the SoC with MSEs of 5.37 to 9.22% and 4.03 to 7.37%, respectively. The promising results can lead to excellent monitoring and control of battery management systems.

1. Introduction

High oil costs, society's growing ecological awareness, and the increased market share of electric and hybrid vehicles have pushed up the demand for clean and sustainable energy [1–3]. On the other hand, many countries have adopted binding regulations to limit the emissions of greenhouse gases into the atmosphere. These rules and regulations have resulted in significant investments and implementations of Renewable Energy Sources (RESs) projects that provide a stable and economical source of power while also protecting the environment. According to Lucchese et al., [4] RESs have contributed to more than half of the capacity of the power sector in more than 140 nations since 2011. Although renewable energy sources have numerous advantages, their output is intermittent and dependent on climate conditions, which are often unpredictable and thus affect the electrical system's reliability and stability. The utilization of Energy Storage Systems (ESSs) is a creative and unique way to tackle these problems and establish a balance between different factors such as electricity generation and demand, improve power quality, and reduce the cost of electricity.

The ESSs in conjunction with Distributed Generational (DG) resources are expected to play an important role in future grids [5,6]. In this respect, Battery Energy Storage Systems (BESSs) is one of the most promising developing ESS technologies for boosting power factor while maintaining reliable supply. To keep the BESSs reliable, safe, healthy, and performing well, some battery parameters, (e.g. State of Charge, SoC) must be monitored in real-time. The SoC is expressed as a percentage of available current capacity divided by nominal capacity. The SoC reflects the remaining capacity inside the battery to prevent overcharging, over-discharge, and damage, as well as to maximize battery longevity [7]. Accurate estimation of the SoC is a sophisticated process due to complicated electrochemical reactions inside the battery, high time variance, and the non-linear relationship between the SoC and the battery parameter (e.g., ambient temperature) [8]. In addition, since the SoC is not a physical entity direct measurement of this value is not possible.

Lookup Table Ways (LTWs), Coulomb Counting (CC), Model-Based Approach (M-BA), and Data-Driven Methods (DDMs) can be utilized to estimate the SoC. Although LTWs are classic and direct methods for

* Corresponding author.
E-mail addresses: e.maita@ttu.edu.jo (E. Almaita), Saleh.alshkoor@emrc.gov.jo (S. Alshkoor), Emad.Abdelsalam@htu.edu.jo (E. Abdelsalam), Falmomani@qu.edu.qa (F. Almomani).

https://doi.org/10.1016/j.est.2022.104761
Received 30 January 2022; Received in revised form 30 March 2022; Accepted 25 April 2022
Available online 12 May 2022

estimating the SoC by leveraging a direct mapping relationship between the SoC and the battery's external properties (e.g. voltage and impedance), they are not ideal for online real-time SoC estimation. This is because the LTWs required separating the load for an extended time to find the relationship between the Open Circuit Voltage (OCV) and SoC [6,9].

The CC is a simple approach for estimating the SoC that involves integrating the discharging current over time. However, its accuracy is dependent on the accuracy of the current sensor used to measure the current value. As a result, any tiny error in the current measurement will result in a big error in SoC estimation. The accumulation of inaccuracies generated by the integration of the current overtime causes this mistake in the current measurement. As a result, this method can not be utilized alone and should be used in conjunction with other methods, limiting its practical application for real-time [9–11]. Electrochemical Model (EC) [12], Equivalent Circuit Model (ECM), and Electrochemical Impedance Model (EIM) [13] are three M-BA approaches that have gained popularity in recent years. The battery models are stated as state equations in these approaches, and adaptive filters and observers are commonly utilized to increase accuracy and reduce uncertainty in open-loop estimating methods [14]. However, because operational factors such as aging, ambient temperature, and environmental factors alter the values of model parameters, there will be higher estimation uncertainty.

When compared to traditional and model-based estimate approaches, DDMs that involve vector machines [15], fuzzy logic [16], and Neural networks (NNs) show significant advantages. DDMs were identified as the best ideal algorithm for accurately predicting the behavior of various linear and non-linear systems. In general, the accuracy of predictions for certain output functions is determined by the input data points. This is done by combining and reasoning the process element's impact on the output function [17–20]. As a result, the DDMs methods are reliant on gathering data that can be fed into the model to build a mathematical link between the input data (ID) (i.e., process parameters) and the output data (OD) without the requirement for a prior physical relationship. Therefore, these methods can be successfully employed for accurate real-time estimation of the SoC in complex battery structures without the need for omitting important details. The neural networks (NNs) method is the most powerful tool for data-driven techniques. This is because it is simple, robust, accurate, and has a parallel processing capability. Nodes termed neutrons connect the independent and dependent parameters within the process to generate the OD. The transfer function (TF) allows each neutron to receive one or more input signals (IS) to contribute to the output signal during this process (OS). Besides that, the training time has shortened from days to hours as a result of the growth in computing power from Graphics Processing Units (GPUs) [21].

Previous studies on SoC measurements have selected the current, voltage, and temperature as ID and the predicted SoC as OD [22,23]. Various types of NNs can be used to estimate the SoC of batteries including Feed-Forward Neural Network (FFNN), Recurrent Neural Network (RNN), and long short-term memory (LSTM). Although the FFNN provides advantages in machine learning by allowing data to be processed independently by several neurons to achieve accurate moderation in a short time, the loss of neighborhood information and the need for more parameters to optimize limit the method's accuracy. Conventional RNN algorithms, on the other hand, performed well when dealing with time-series data because they capture the battery's nonlinear dynamic performance due to its ability to retain past information [24,25]. Nonetheless, one of the major drawbacks of the RNN is its incapability of handling long-term dependency during the training phase. This drawback could be influenced by past inputs, fades out exponentially, and causes the problem of gradient vanishing or exploding phenomena. To resolve this problem, Hochreiter and Schmidhuber suggested a long short-term memory (LSTM) solution with an adaptive “forget gate” that allows an LSTM to learn to reset itself at opportune moments, thus freeing up internal resources [26].

Many researchers have used the LSTM methodology to estimate SoC and discovered that it outperforms other NN methods, especially in situations where continuous real-time SoC estimates for batteries connected in series are required. It was highlighted that the LSTM has an excellent ability to capture the long-term dependencies and the dynamic changes in the battery. Yang et al., [21] suggested a combination of an LSTM -RNN and Unscented Kalman Filter (UKF) to model battery behaviors and estimate the battery SoC under varying temperatures using voltage, current, and temperature as an ID. The developed model showed a good tendency to correlate the battery SoC to the change in temperature in the range of 0 to 50 °C. The model prediction was excellent with an RMSE $\leq$1.1% and mean average errors (MAR) $<$ 1%. Bockrath et al. [27] examined the performance of LSTM and equivalent circuit model (ECM) coupled with Kalman Filters (EKF) in estimating the SoC for lithium-ion batteries (LIB) under real conditions. It was confirmed that the self-learning ability of the data-driven LSTM method could predict the non-linear behavior of LIB under different environmental and working conditions throughout the battery life. LSTM approach showed better accuracy and stability under dynamic loading profiles. The result shows that the ECM- EKF achieved an RMSE of 9.5%, whereas the LSTM achieves an RMSE of 5.0%. Yang et al. [28] proposed a method that uses the LSTM network to model the complicated dynamics of LIB and determine the SoC using voltage, current, and temperature as an ID. The results of the model-based filtering strategy (unscented Kalman filter) are compared to the results of SOC estimation in terms of tracking accuracy, computation time, and resilience against unknown initial states. The findings show that this method captures the nonlinear relationship between SoC and input values and has greater tracking accuracy than the UKF, where the RMSE and MAR were within 2% and 1% of the incorrect initial SoC, respectively. Mamo and Wang [29] showed that the LSTM model can be accurately used to estimate the charging status of two LIBs. The LSTM based on the attention mechanism provides accurate and stable estimation, compared with classic LSTM and other types of machine learning methods (RNN, SVM, ANN). The proposed method performs best compared with published methods such as SVM, standard RNN, LSTM, SVM-PF, standard RNN-PFs and showed excellent performance at three temperatures 0, 25, and 40 °C with an RMSE of 0.9593, 0.8714, and 0.9216, respectively. Research works that present the estimation of SoC for battery packs are limited. Shu et al., [30] confirmed that due to differences across battery cells, creating a reliable assessment of the SoC of LIB packs remained difficult. To address this issue, they propose estimating the pack SoC using a combination of an enhanced square root-cubature Kalman filter (SRCKF) and a multi-innovation smoothing approach. Experimental data under time-varying temperature settings were used to verify the model's robustness and accuracy, as well as the cell SOC estimation. The experimental findings show that the SoC estimation error may be kept to less than 2%. Chen et al., [31] estimated the SoC for a series battery pack using LSTM-RNN combined with the design of an intelligent equalization charging system. In this system, the charge equalization was established using a 40 Ah lithium battery. Although the study found that once the primary charger stops producing current, the auxiliary constant current source could continue to charge the remaining batteries that are not fully charged, the time and charging efficiency were not examined. The capacity of some batteries after charging and discharging, as well as inconsistencies, were not mentioned. Wong et al., [32] showed that using a deep LSTM is a useful way to determine the SoC over two LIB datasets. It was concluded that LSTM predicts the SoC of cylindrical LIB under different charge-discharge cycles. A real-time SoC determination of lithium battery packs cells (1300 mAh) using a Multi-layer Neural Network (MNN) and LSTM was suggested by Park et al. [33].

The previous literature review shows that most research works focus on the estimation of SoC for one battery or battery cell used in electrical vehicles and the research work on packs of batteries is limited, which is not practical to be employed for RESs. There is acknowledge gap and a need for establishing an accurate method that can be used to estimate

the SoC for the grid-scale battery storage system. Most of the published works are based on developing a complicated system consisting of cubature Kalman filter coupled with an intelligent equalization charging system to obtain accurate results. Other models required two types of datasets: a voltage dataset and a combined voltage and temperature to achieve accurate prediction [33]. In addition, most of the previous work focused on applications with lower battery capacity and focused only on discharge cycles [32]. Therefore, this will be the first work that focused on developing a protocol to estimate the SoC for the grid-scale battery storage system. The proposed estimation process is simple and based on one stage of estimation using the LSTM, and deployed 10 batteries that have large capacity (2100 kWh and 2187 Ah). Instantaneous value of ambient temperature (T_{amb}), DC bus voltage (DvBV), DC bus current (DvB*i*) were used as an ID for the newly developed model to estimate the SoC based on real data considering the effect of the operating conditions and the charging-discharging process. The results of the LSTM models were compared with conventional Feed- FFNN and DFFNN models considering both charging and discharging cycles.

2. System description and data generation

2.1. System description

The data utilized to train, validate, and NN models were obtained from the Al-Manara PV power facility in Jordan, which is the first to use a BESS. The power plant has a 12 MWh battery storage system that is connected to the Irbid District Electricity Company (IDECO). The system is connected to Sabha and Alsalhiah villages and provides medium voltage network feeders with 33 kV for each village, with a system storage capacity of 2 MW and 1 MW, respectively, and the discharge period is 4 h. Fig. 1 shows the single-line diagram of the Al-Manara PV power plant. This power plant has been commercially operated since 2015, with a 23 MWp, 18 MVA capacity, and a limited 13 MW AC output at the Point of Common Coupling (PCC). The maximum AC threshold values at the PCC are 8, 4, and 1 MW supplied to Sabaha, Alsalhyia, and Safawi feeders, respectively.

2.2. Data generation and preparation

The data was collected every 15 min, starting at 12:00 AM until 11:45 PM on a daily bases from April 2020 until September 2020. The number of data points collected during this period was 17,280, which were decreased to 15,373 data points after cleaning. The ID consists of dc bus voltage (DvBV), dc bus current (DvB*i*), and the ambient temperature (T_{amb}), while the OD is the calculated SoC for the battery pack. Figs. 2 and 3 show samples of ID and OD for April and May, respectively.

To validate the discharge period (4 h) of this system, the ID (DvBV, DvB*i*, and T_{amb} with the corresponding values of SoC as OD were averaged and represented for one day. Fig. 4 shows an example for the discharge period in May, it was observed that the discharge period is spanning in the range of 960 to 1200 min (i.e. over 240 min, which represents 4 h of discharge time.

3. SoC estimation methods

3.1. LSTM neural network

3.1.1. LSTM cell construction

The LSTM is the proposed to estimate battery SoC, due to its capability to transact with multi-dimensional data without any previous knowledge of the battery model. In other words, the LSTM is capable to generate a mathematical relationship that correlates the ID (DvBV, DvB*i*, and T_{amb}) to the OD (SoC) without the need for a prior physical relationship. Additionally, a key feature of the LSTM is its capability in learning long-term dependencies between time steps of sequence data [34]. The LSTM consists of one cell state located in the horizontal line at the top of the structure and three gates (input gate, output gate, and forget gate) that read and write the cell state as shown in Fig. 5. The gates are made up of several neurons that have been trained to decide which information to forget or remember and retrieve in order to get the output based on the previous output and the current input.

The forget gate is responsible for determining what information should be remembered or ignored from the previous cell state. This is done by the sigmoid function, which takes the (h_{t-1}) and (X_t), and the outputs from it is a number between 0 and 1 for each number in the cell state (C_{t-1}). Therefore, the output (ft) of the forget gate is determined by Eq. (1):

$$ft = \sigma\left(Wf.[h_{t-1}, X_t] + bf\right) \tag{1}$$

Where σ is a sigmoid activation function defined as

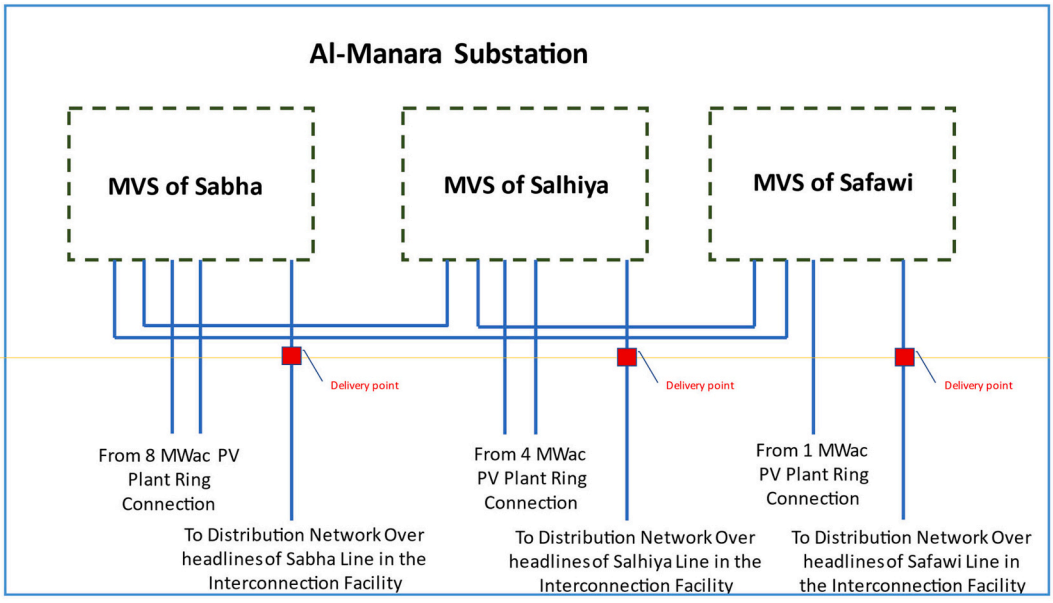

Fig. 1. Single line diagram of the Al-Manara PV substation.

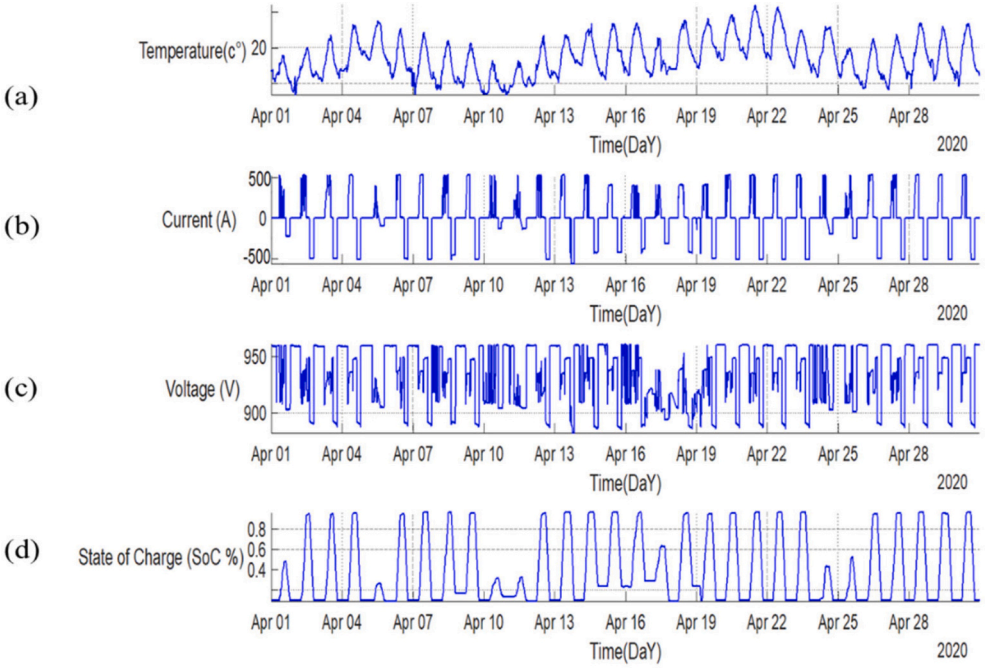

Fig. 2. The ID, (a) dc bus voltage (DvBV), (b) dc bus current (DvB*i*), and (c) the ambient temperature (T_{amb}) with the corresponding SoC values as OD during April.

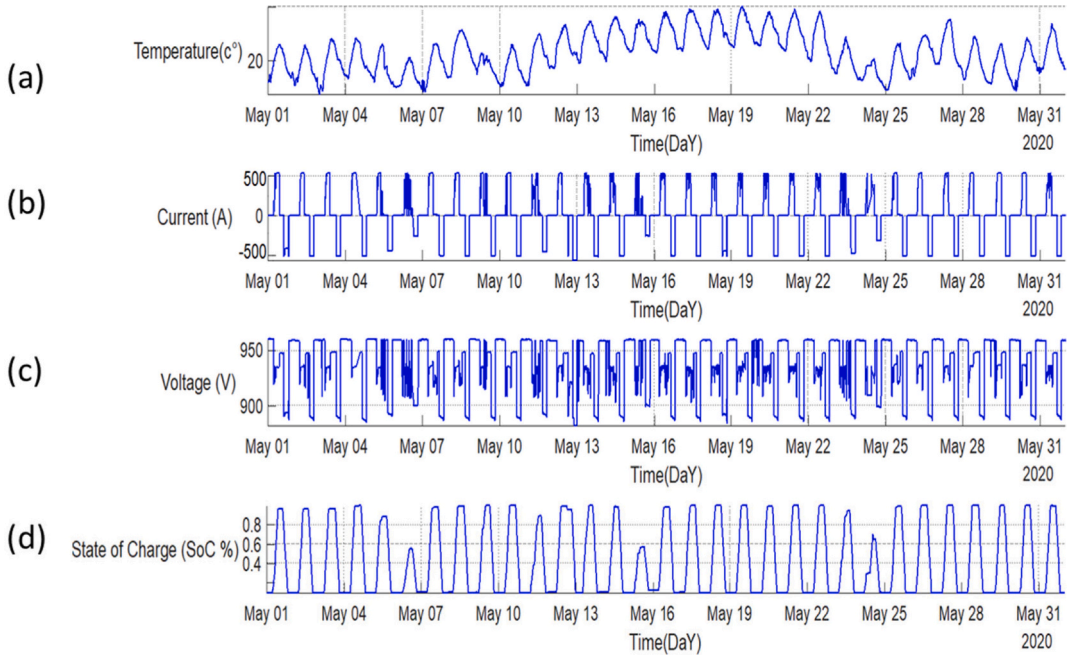

Fig. 3. The ID, (a) dc bus voltage (DvBV), (b) dc bus current (DvB*i*), (c) the ambient temperature (T_{amb}), and (d) the corresponding SoC values as OD during May.

$$\sigma = \frac{1}{1+e^{-x}} \tag{2}$$

The output of the sigmoid function is restricted between 0 and 1, which means that the LSTM can be explained as a forgetting factor. In other words, the sigmoid function act as a filter in the model-based approach to accepting or rejecting the calculated value. The next step is deciding what new information to remember (store) in the cell state. This is done by using two steps; the first step uses a sigmoid function in the input gate to decide which values will be updated (i.e generating values for i_t), while the second step uses a tanh function to create a vector of new candidate values, C_t', that could be added to the state. After that, the combination of two vectors is used to create an update value to the state. The outcome of both steps (i_t and C_t') can be determined using Eqs. (3), (4), respectively.

$$i_t = \sigma\left(Wi.[h_{t-1}, X_t] + bi\right) \tag{3}$$

$$C_t^{'} = tanh\left((Wc.[h_{t-1}, X_t] + bc\right) \tag{4}$$

Where the tan hyperbolic function is.

$$tanh = \frac{e^{x} - e^{-x}}{e^{x} + e^{-x}} \tag{5}$$

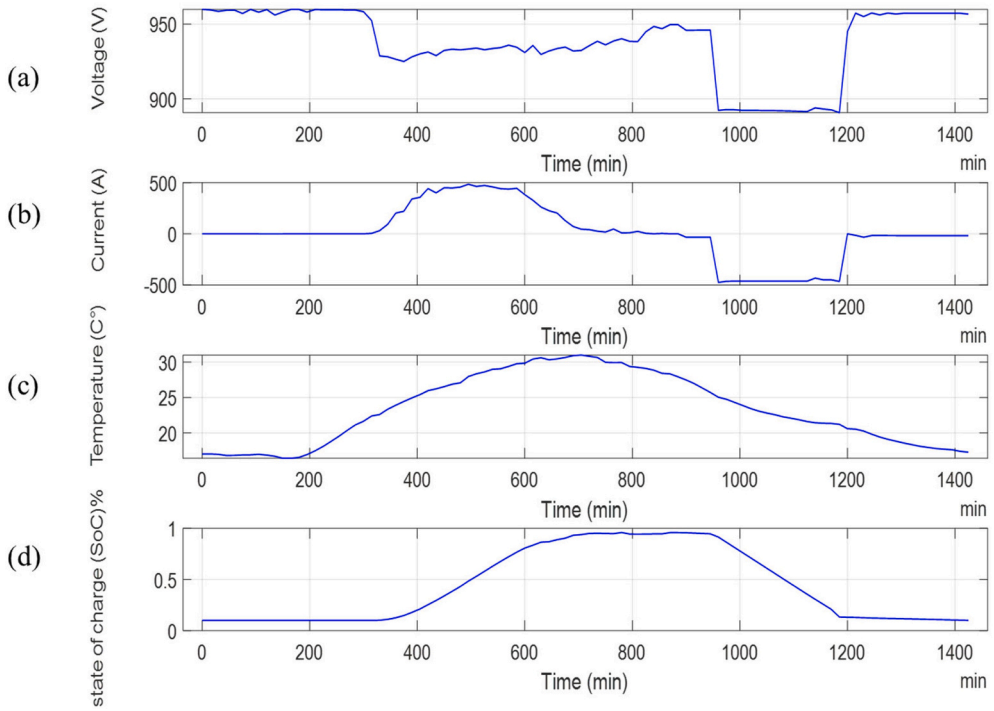

Fig. 4. Average of the ID (a) DvBV, (b) DvB*i*, and (c) T_{amb} with the corresponding SoC (d) during May.

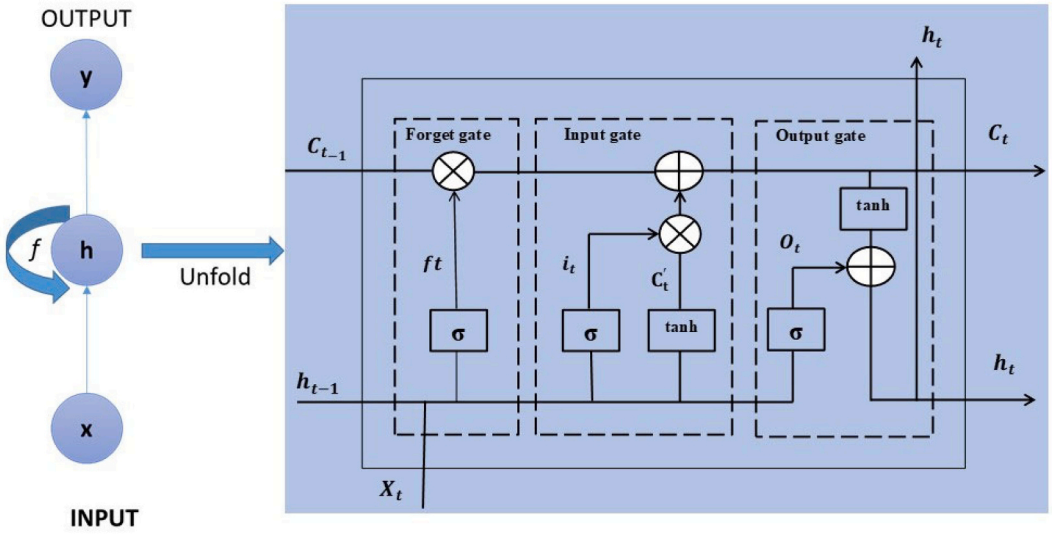

Fig. 5. Unfold Structure of the LSTM cell.

Following the determination of the old cell state and the appropriate decision on what information should be remembered or forgotten, the values of (C_{t-1}) is updated into the new cell state (c_t). The new cell state was determined by multiplying the old state C_{t-1} by f_t factor and then added to the value of i_t * C_t' as per Eq. (6). The new cell state can be determined using Eq. (6):

$$C_t = ft{*}C_{t_{-1}} + i_t{*}C_t^{'} \tag{6}$$

The final step is to determine the output dada (O_t) based on the cell state The calculated values were first filtrated using the sigmoid function to decide what values of the cell state are to be reported or ignored, Eq. (7). Then, an additional tanh function is used to push the output values between −1 and 1 as in Eq. (8)

$$O_{t=}\,\sigma\,(Wo.[h_{t-1}, X_t] + bo\,) \tag{7}$$

New hidden State:

$$h_t = O_t.tanh(C_t) \tag{8}$$

3.1.2. *Proposed LSTM method for SoC estimation*

The configuration of the LSTM network used for the estimation of the SoC is presented in Fig. 6. The LSTM network starts with a sequence input layer (IL) that takes the ID (DvBV, DvB*i*, and T_{amb}) vectors to calculate the values of SoC as an OD. The output vector of the LSTM layers is routed through a fully connected layer to the output layer for regression to estimate the SoC value.

At each time step, a forward pass begins just after the training dataset

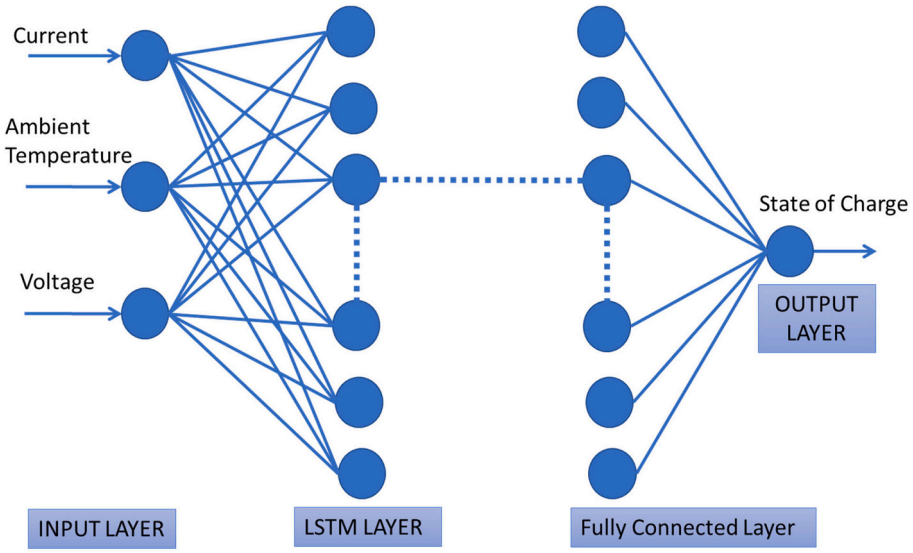

Fig. 6. The architecture of simple LSTM network for regression.

is received in the network and ends when an accurate value of SoC is calculated. The error and the overall loss are also calculated. The Adam optimizer is used to update the values of weights and biases in the backward pass [35].

Typically, the training phase consists of more than one batch. Each patch has one forward and one backward pass to ensure that each sample contributes to the updating of internal network parameters. This approach is repeated indefinitely to update the weights and biases until the desired convergence criteria is achieved. The precise model parameters of the proposed LSTM network for the SoC estimate are shown in Section (IV-A).

3.2. Feed-Forward Neural Network (FFNN) & Deep-Feed-Forward Neural Network (DFFNN)

The conventional FFNN is presented in Fig. 7. Because of its simplicity, the FFNN is regarded as one of the most fundamental ANN algorithms. The training of this algorithm is a one-way process that only moves forward.

The conventional FFNN has three layers, namely, the input layer (IL), hidden layer (HL), and an output layer (OL). The IL usually takes the instantaneous values of ID (DvBV, DvB*i*, and T_{amb}) and determines the OD via the OL as an instantaneous SoC value (SoC_i). The processing of the ID to OD is made of several processing units called neurons interconnected with each other.

$$SoCi = fi\left[\sum_{k} Wj,k \times Oj + \theta j,K\right] \tag{9}$$

where *Wj*; *k*, *θj*; *k* denotes the weight and bias from the HL to OL, respectively. *Oj* refers to the output of the HL, and *fi* refers to the activation function. The DFFNN is done by adding another HL to the conventional FFNN. As the distribution of weights, which are determined by optimization with the training data set might exhibits invariant for the large number of nodes. Adding additional HL will help minimize the error and improve the prediction of the SoC values. More details about FFNN and its classification preprocessing techniques in [36,37].

3.3. The criteria used for quantitative comparisons of different SoC estimation methods

The estimated SoC values by different methods in comparison with

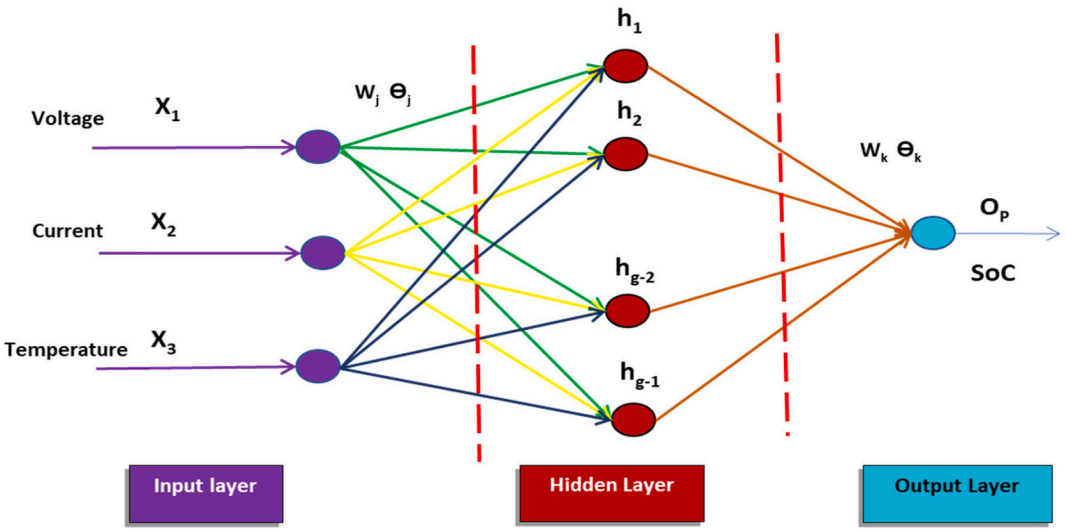

Fig. 7. Conventional FFNN Structure.

real values were assessed using the maximum standard error (MSE), and root mean square RMSE as per Eqs. (10), (11)

$$RMSE = \sqrt{\frac{1}{n}\sum_{i=0}^{n}(true\ value - predicted\ value)^2} \quad (10)$$

$$MSE = \frac{1}{n}\sum_{i=0}^{n}(true\ value - predicted\ value)^2 \quad (11)$$

The true values refer to the real data of the SoC and the predicted values refer to the output values obtained from the SoC estimation method. The real SoC values were obtained from the battery management system in the Al-Manara PV power facility. Tesla, the manufacturer of the lithium-ion battery packs, supplied this measurement system.

4. Experimental design and results

4.1. Models parameters

A MATLAB® software and a PC with a core i7 CPU were used in system training and testing. The data were cleaned and normalized between (-1, 1). The cleaning and normalizing of the data are very crucial steps to boost the performance of the neural networks topologies. The data were separated into the training and testing. The ID used in the training set represents 70% of the data points, while 30% of the data points were used in the testing set. The number of HLs is one (1) with 22 neurons, the learning rate of 0.01, and the number of epochs of 150. The ID (DvBV, DvB*i*, and T_{amb}) were read by the LSTM, FFNN, and DFFNN topologies and used to estimate the SoC as an OD. The results from the LSTM topology were compared with values determined by FFNN and DFFNN. The estimation of the SOC of a battery pack was considered a time series problem. Therefore, a correlation between the input's instants and the output instant parameters was carried out to get the most accurate results. The parameters instants that have the best correlation factor with the OD (SOC) are presented in Table 1. For example, for the model number (1) in Table 1, the models' inputs are T_{amb} denoted by k-2, DvB*i* denoted by k-5, and DvBV denoted by k, while the OD is SOC denoted by k. The three different models shown in Table 1 were used to test each of the NN topologies (LSTM, FFNN, and DFFNN) and the results were summarized in the next sections. The cost functions used to evaluate the performance of each topology are RMSE and MSE, which are the most common cost functions used in literature.

4.2. Results and discussion

4.2.1. SoC estimation using FFNN and DFFNN

The FFNN topology with one HL, 22 neurons, the learning rate of 0.01, and the number of epochs of 150 was trained and tested to estimate the SoC of lithium-ion battery packs. The estimation process used three different models mentioned in Table 1. The RMSE and MSE of the three different FFNN models are presented in Table 2. The three models could be used to estimate the SoC of lithium-ion battery packs with an RMSE in the range 0.23182 to 0.30357, and MSE in the range 0.0922 to 0.0537. However, model number (3) has the best performance with RMSE and MSE of 0.23182 and 0.0537, respectively.

The results indicated that the architecture and model of the NN have an important effect on the SoC estimation accuracy. The results also highlight the importance of the correlation methodology in minimizing the error in SoC estimation. Out of the three studied models, model number (3) showed has the best correlation factor that uses the ID to determine the OD with a minimal error. Fig. 8a and b present the observed versus estimated SoC as well as the reported error for 15,373 data samples used in FFNN. The FFNN topology has a good performance in estimating the SoC as shown in Fig. 8a. It was observed that the estimated SoC is in good agreement with the real SoC all over the tested data samples. Up to 85% of the tested sample points have an error between the estimated and observed SOC within ±0.5 (see Fig. 8b). This confirms that the use of topology and model can moderately determine an accurate value of SoC. To gain a better understanding of the results in Fig. 8, a zoom-in for one-week and one-day performance periods for the same figure were plotted in Figs. 9 and 10, respectively. Both figure to demonstrate that the estimated and measured SOCs varied significantly and more improvements in the NN structure are required to achieve lower error and better estimation. Even though the FFNN has advantages in machine learning by allowing data to be processed independently by several neurons to achieve accurate estimation for SoC in a short time, the method's accuracy is still limited. This is due to the loss of neighborhood information and the need for more parameters to optimize or the need for higher numbers of Epochs.

The second topology used in estimating the SoC is the DFFNN. This topology has the same ID and OD as the FFNN but with an additional HL (i.e. two HLs in total). The learning rate and the number of epochs were set the same. The topology was trained and tested using the three different models mentioned in Table 1 and the obtained RMSE and MSE were summarized in Table 3.

The three models showed better accuracy in estimating the SoC compared to FFNN. The RMSE and MSE were in the range 0.20078 to 0.27143 and 0.0403 to 0.0737, respectively. Model number (3) still shows the best estimation performance with RMSE and MSE of 0.20078 and 0.0737, respectively. The results show improvement over the conventional FFNN. The additional HL has a direct role in importing the values of the SoC, by refining the feedforward-back propagation of the NN. Fig. 11a and b present the observed versus estimated SoC as well as the reported error for 15,373 data samples used in DFFNN. The improved DFFNN topology has a good performance in estimating the SoC as the estimated SoC is in good agreement with the real SoC all over the tested data samples (Fig. 11a). Up to 93% of the tested sample points have an error between the estimated and observed SOC within ±0.25 (see Fig. 11b). This confirms that improving the structure of the NN has a significant effect on the prediction of the SoC. Figs. 12 and 13 present a zoom-in for the data point in Fig. 11 for periods of one-week and one-day performance. The differences between the estimated and observed SOC was significantly reduced compared with the results obtained from FFNN. The estimated vs. observed values of SoC are in good agreement. The DFFNN topology can determine the SoC under different ID values. It was observed that in this estimated approach up to 96% of the data are close to real SOC values. The error in most cases ranged between ±0.07. The very small RMSE error between estimated and observed SoC values confirms that the DFFNN model is acceptable and does not have any systematic errors. However, further improvements are still needed to be more generalized. The DFFNN performed well when dealing with time-series data because it captures the battery's non-linear dynamic performance of the battery pack and it has a good ability to retain past information [24,25]. However, one of the major drawbacks of the DFFNN is its incapability of handling long-term dependency during the training

Table 1
Input and output values of the models.

Model number	Value of temperature	Value of current	Value of voltage	Value of SoC
1	K-2	K-5	K	K
2	K-2	K-10	K	K
3	K-2	K-10 and K-3	K	K

Table 2
The Summary of FFNN results in different models.

Model Number	Number of Epochs	RMSE	MSE
1	150	0.30357	0.0922
2	150	0.25577	0.0654
3	150	0.23182	0.0537

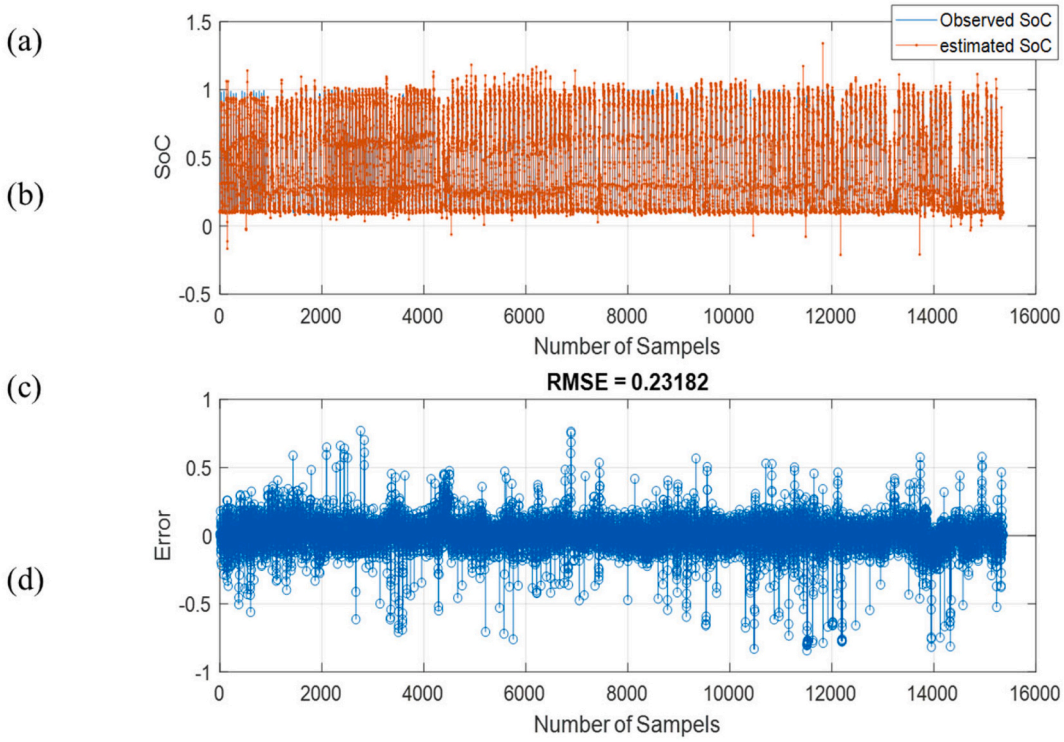

Fig. 8. The performance of model 3 FFNN at 150 epochs: (a) observed and estimated Soc, (b) Error and RMSE value.

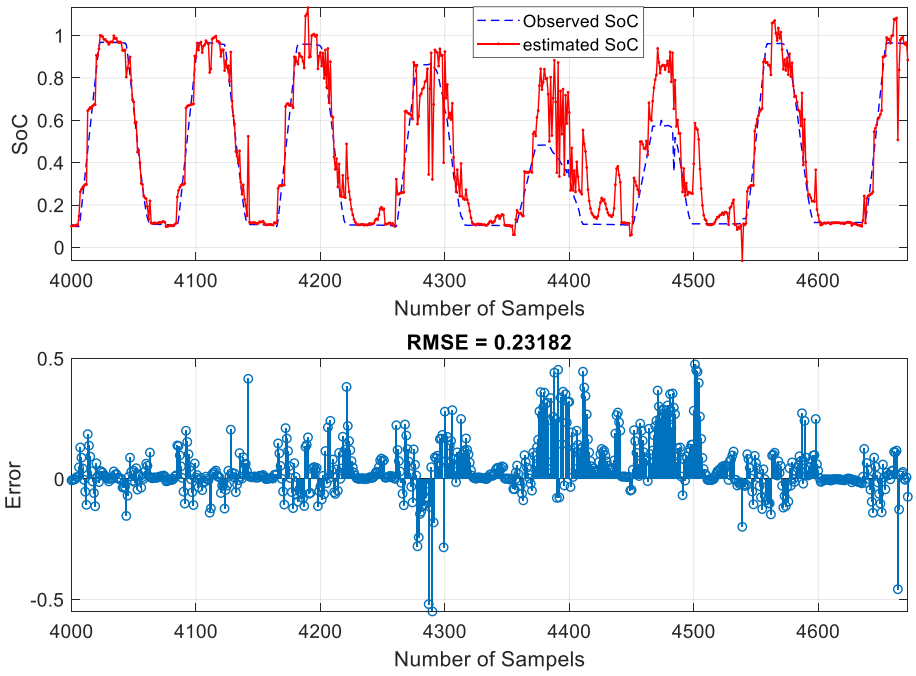

Fig. 9. Zooming for the performance of model 3 FFNN at 150 epochs: one-week performance.

phase. This drawback could be influenced by past inputs, fades out exponentially, and causes the problem of gradient vanishing or exploding phenomena.

4.2.2. SoC estimation using LSTM

The LSTM was tested as the third topology with parameters similar to the previous two topologies. This topology has one (1) HL, 22 neurons, a learning rate of 0.01, and e number of epochs of 150. The same previous models were used in training and testing. Table 4 summarizes the RMSE and MSE from the three different models. The LSTM exhibited excellent performance in estimating the SoC. For the three models, the RMSE and MSE for the estimates SoC did not exceed 0.078574 and 0.0062, respectively. Moreover, model number (3) has the best performance with RMSE and MSE of 0.069539 and 0.0048, respectively. The LSTM with characteristics to learn and adapted to the training date as well as using the concept "forget gate" showed excellent ability to determine the

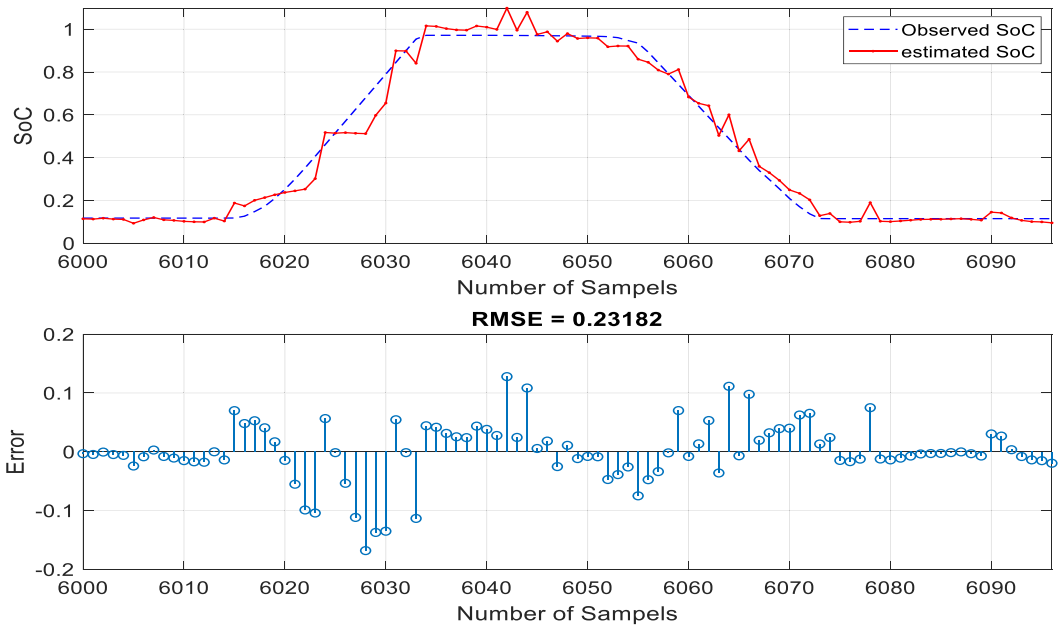

Fig. 10. Zooming for the performance of model 3 FFNN at 150 epochs: one-day performance.

Table 3
Summary of the DFFNN results for the different models.

Model Number	Number of Epochs	RMSE	MSE
1	150	0.27143	0.0737
2	150	0.23146	0.0536
3	150	0.20078	0.0403

SoC under different ID data. This characteristic allows the LSTM to learn and reset itself at opportune moments, thus freeing up internal resources. Therefore, this method could be considered superior in terms of self-training and correction. Fig. 14a and b present the observed versus estimated SoC as well as the reported error for 15,373 data samples used in LSTM. The estimated SoC is in good agreement with the real SoC all over the tested data. Up to 99% of the tested sample points have an error between the estimated and observed SOC within ±0.03. Confirming the superiority of this structure in the prediction of the SoC. A zoom-in of the tested data points periods of one-week and one-day (Figs. 15 and 16) showed that the LSTM exhibited excellent follow-up to the real SoC

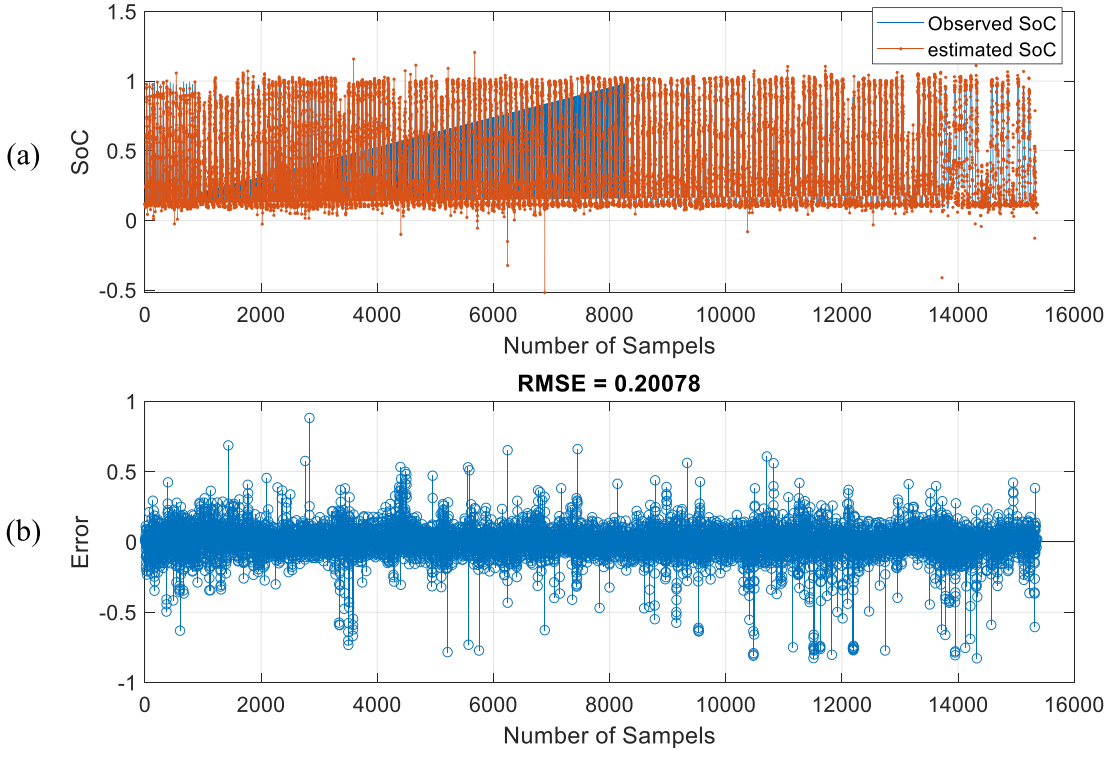

Fig. 11. The performance of model 3 DFFNN at 150 epochs: (a) observed and estimated SoC, (b) Error and RMSE value.

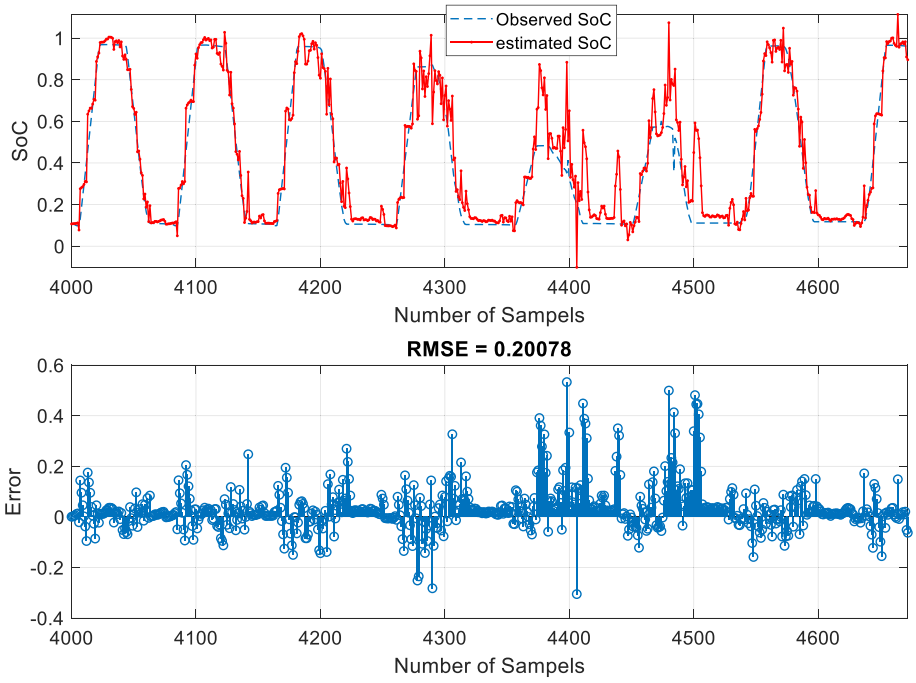

Fig. 12. Zooming for the performance of model 3 DFFNN at 150 epochs: one-week performance.

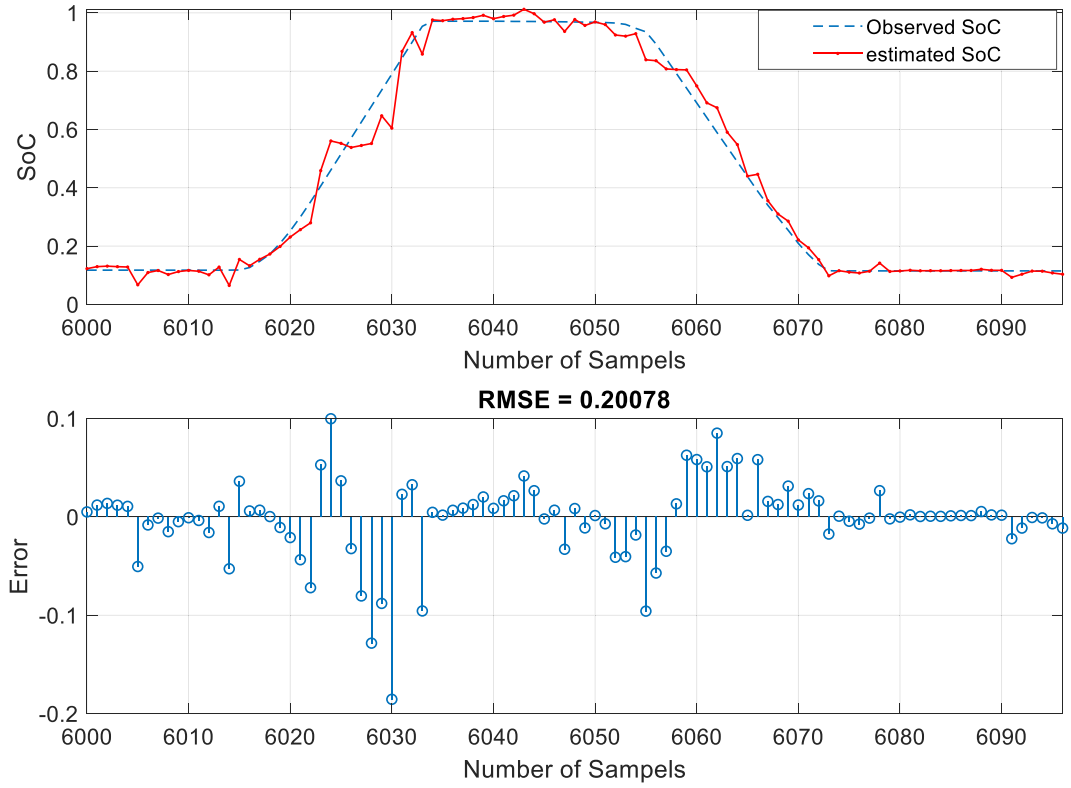

Fig. 13. Zooming for the performance of model 3 DFFNN at 150 epochs: one-day performance.

Table 4
The results of the LSTM for the different models.

Model number	Number of Epochs	RMSE	MSE
1	150	0.078574	0.0062
2	150	0.077138	0.0060
3	150	0.069539	0.0048

values. The differences between the estimated and observed SOC was not observed. Under all the tested ID values the residual error is no more than ±0.03. The results also show that the LSTM topology deals very well with the influence of different operating conditions, and it can learn the dynamic behavior of a group of batteries better than the FFNN and DFFNN methods. The LSTM showed an excellent ability to capture the long-term dependencies and the dynamic changes in the battery,

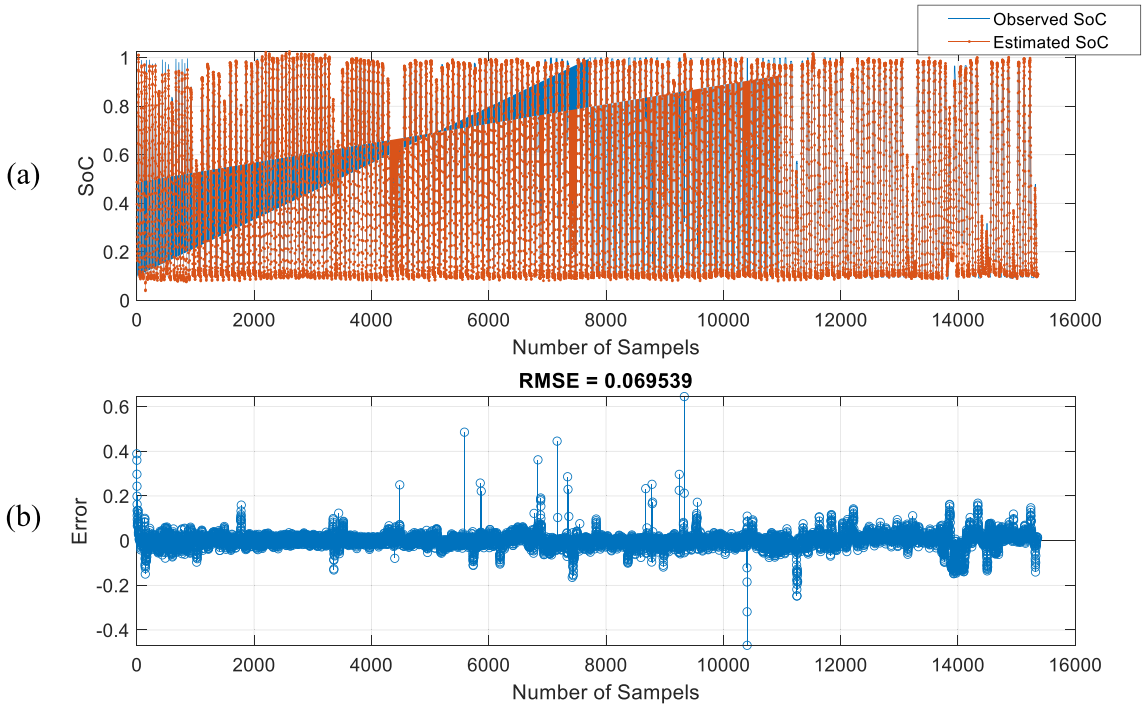

Fig. 14. Performance of model 3 LSTM at 150 epochs: (a) observed and estimated SoC, (b) Error and RMSE value.

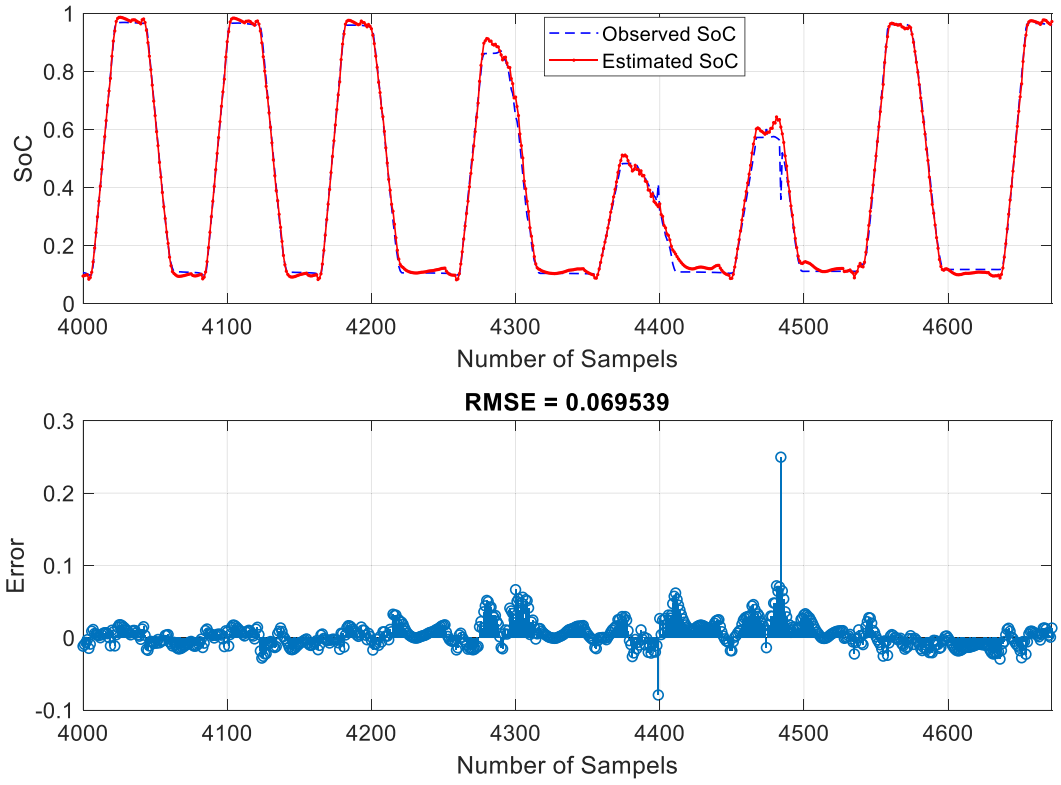

Fig. 15. Zooming for the performance of model 3 LSTM at 150 epochs: one-week performance.

especially in situations where batteries are connected in series as well as batteries with high capacity. Moreover, the LSTM does not require two types of datasets as with other NN.

Fig. 17 summarizes the performance of the three different network architectures in estimating the SoC of the packed lithium batteries. While the FFNN and DFFNN gave a reasonable estimate for the SoC with an MSE in the range of 5.37 to 9.22% and 4.03 to 7.37%, respectively, the LSTM accurately estimated the SoC with an MSE no more than 0.62% for all the three models. Under the same conditions, the LSTM is the best and most accurate method. In addition to its ability to learn and reset itself at opportune moments, the LSTM can achieve reasonable results at lower epochs. FFNN and DFNN, in particular, may require

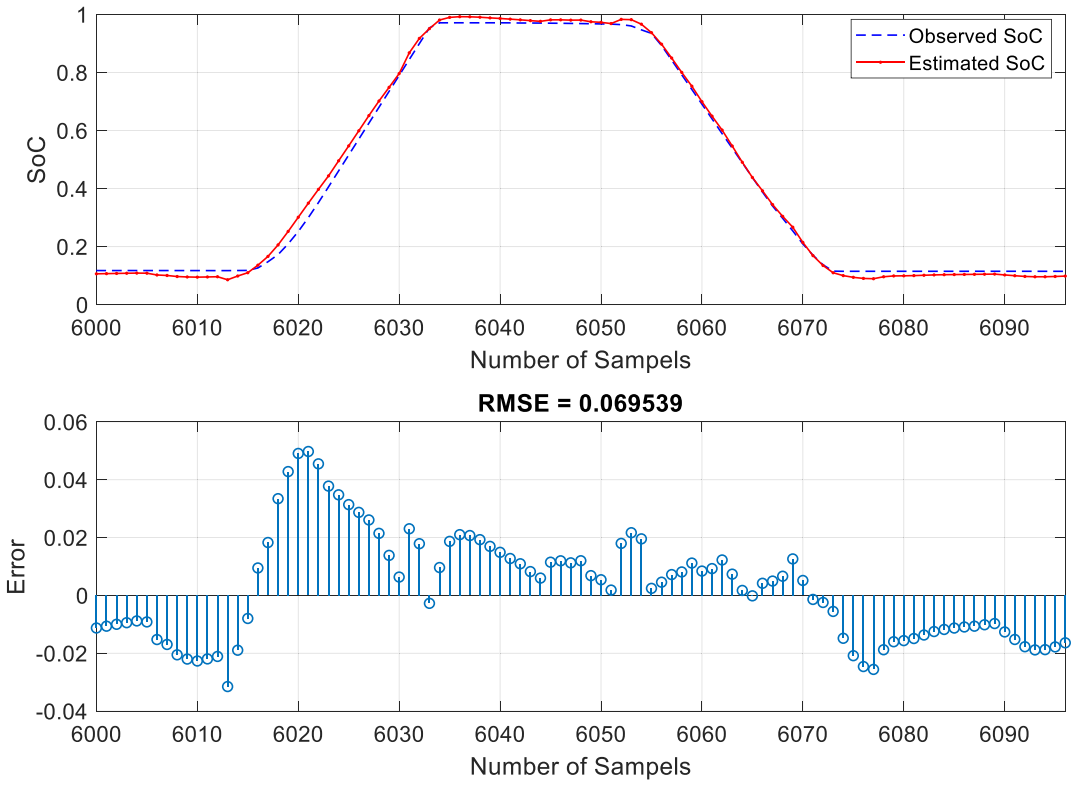

Fig. 16. Zooming for the performance of model 3 LSTM at 150 epochs: one-day performance.

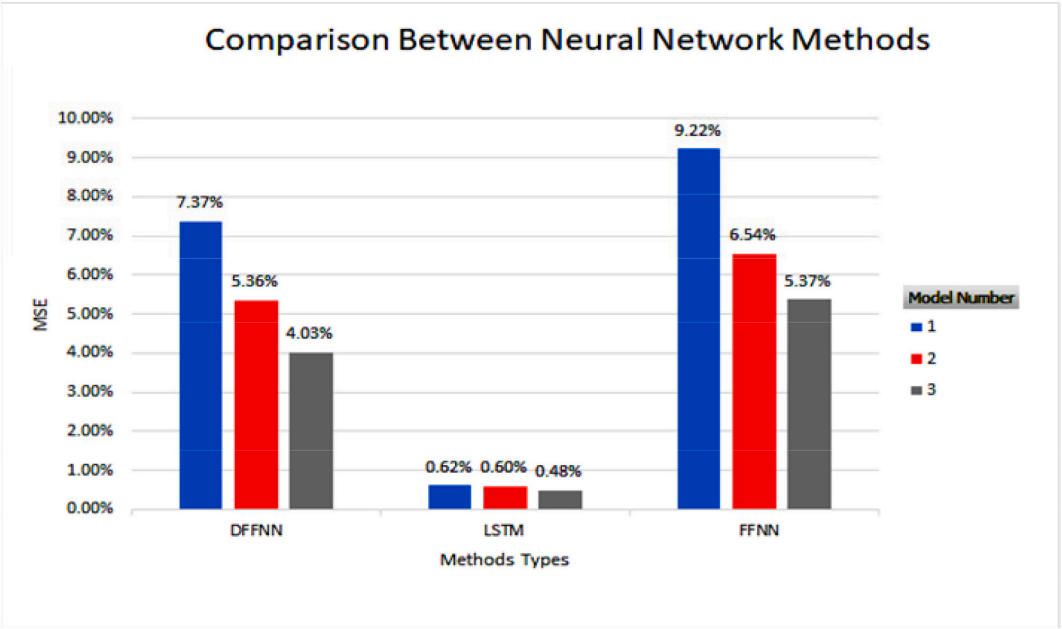

Fig. 17. Comparison between neural network methods -MSE Values.

more time and epochs to converge at a reasonable RMSE. According to previous research, the most obvious difference between LSTM, DFFNN, and FFNN is the number of epochs required for training. While the LSTM achieved accurate SoC estimation, other network architectures may need more epochs to achieve reasonable accuracy, despite having less computational complexity per time step. The differences in SoC estimation could be explained by the fact that the FFNN and DFFNN require more fine-tuning of their weights to access long-range contextual information. LSTM, on the other hand, benefited more from longer target delays than other network architectures because it has the greater capability with long time lags, allowing it to use the extra context without suffering as much from having to store previous inputs throughout the delay. As a result, LSTM demonstrated an exceptional ability to store and access information over very long periods. The LSTM networks were not only faster but also more accurate. The fact that the difference between the real and estimated SoC is not large could simply mean that this task does not require very long time dependencies. Interestingly, LSTM with no time delay produces nearly identical results,

implying that the ability to learn is critical.

The SoC estimation accuracy of the current study is slightly higher than the work of Chen et al., [23]. While the LSTM showed an error in the range of ±0.03% the prediction error in the work of Chen et al., [23] ranged from 1 to 4%. In addition, the previous work focused on a primary charging battery while the other remaining batteries start to charge in the secondary stage, which might increase the charging time. In the present study, the charging and discharging of the pack of the battery were proposed as a unit to minimize the time and increase the energy. The work of Wong et al., [24] on the other hand reported an effective LSTM NN is a useful way to determine the SoC over two LIB datasets. The NN architecture required during the training stage 1000 epochs to achieve estimation efficiency with RMSE in the range of 1.47 to 2.73% depending on the number of steps in each model. Therefore, the accuracy of the present work considers better under lower number of epochs. Comparable results were reported by Park et al. [25] who estimated the SOC of lithium battery, using the cubature Kalman filter method with a maximum error of 3% under different temperatures.

5. Conclusion

In this paper, the SoC for a grid-scale lithium-ion battery storage system was estimated using three different NN models (FFNN, DFFNN and LSTM). Real data from the Al-Manara PV power plant in Jordan, was used to train and test the models and detailed data preprocessing and features selection procedures were demonstrated. The performance of the NN models for the three different time series models. This preprocessing phase leads to three different time series models with an ID of T_{amb}), DvBV, and DvB*i*. The LSTM neural network model with the ability to learn to overcome the complexity and uncertainty of the estimation process. Results showed that the LSTM accurately estimated the SoC with an MSE of no more than 0.62% for all the three-time models, while the FFNN and DFFNN gave a reasonable estimate for the SoC with an MSE in the range of 5.37 to 9.22% and 4.03 to 7.37%, respectively. The ability of the LSTM model to learn and reset itself at opportune moments outperforms the accuracy of FFNN and DFNN even under lower number of epochs. The LSTM topology showed an excellent tendency to deal well with the influence of different operating conditions, and it can learn the dynamic behavior of a group of batteries better than the FFNN and DFFNN methods. The reported SoC estimation accuracy is higher than other methods reported in the literature and can be used to implement packed battery systems management strategies with high capacity.

CRediT authorship contribution statement

The corresponding author Prof. Almomani confirms the contributions of the authors to this manuscript were as follows

Eyad ALMaita Conceptualization, Methodology, Modeling, Figures preparation, pre-Writing

Saleh ALShkoor: Conceptualization, Methodology, Modeling, Figures preparation, software, pre-Writing-,

Emad Abdelsalam: Original draft preparation, Data curation, Discussion, Validation, Tables preparation

Fares Almomani Conceptualization, Methodology, Modeling Tables preparation, pre-Writing-, Validation, Tables preparation, Writing- Reviewing and Editing

Data availability

The raw/processed data required to reproduce these findings cannot be shared at this time due to legal or ethical reasons.

Declaration of competing interest

The authors whose names are listed immediately below certify that they have NO affiliations with or involvement in any organization or entity with any financial interest (such as honoraria; educational grants; participation in speakers' bureaus; membership, employment, consultancies, stock ownership, or other equity interest; and expert testimony or patent-licensing arrangements), or non-financial interest (such as personal or professional relationships, affiliations, knowledge or beliefs) in the subject matter or materials discussed in this manuscript.

Acknowledgment

The authors acknowledge the support of Irbid District Electricity Company (IDECO) for providing data, the MERG lab (www.htu.edu.jo/merg), Eng. Hamza Adamat for their support in developing this work. Special thanks to Luz A. Gonzalez for proofreading and editing the manuscript. Authors acknowledge the *open Access funding provided by the Qatar National Library*.

References

[1] M. Sufyan, N.A. Rahim, M.M. Aman, C.K. Tan, S.R.S. Raihan, Sizing and applications of battery energy storage technologies in smart grid system: a review, J.Renew.Sustain.Energy 11 (2019), 014105.
[2] Z. Bouabidi, F. Almomani, E.I. Al-musleh, M.A. Katebah, M.M. Hussein, A. R. Shazed, et al., Study on boil-off gas (BOG) minimization and recovery strategies from actual baseload LNG export terminal: towards sustainable LNG chains, Energies 14 (2021) 3478.
[3] R.Q. Hu, Mobility-aware edge caching and computing in vehicle networks: a deep reinforcement learning, IEEE Trans. Veh. Technol. 67 (2018) 10190–10203.
[4] F.C. Lucchese, L.N. Canha, W.S. Brignol, B.K. Hammerschmitt, L.N. Da Silva, C. C. Martins, Energy storage systems role in supporting renewable resources: global overview, in: 2019 54th International Universities Power Engineering Conference (UPEC), IEEE, 2019, pp. 1–6.
[5] A. Jamali, N. Nor, T. Ibrahim, Energy storage systems and their sizing techniques in power system—a review, in: 2015 IEEE Conference on Energy Conversion (CENCON), IEEE, 2015, pp. 215–220.
[6] B. Zhang, C. Lu, J. Liu, Combination algorithm for state of charge estimation, in: 2013 International Conference on Communication Systems and Network Technologies, IEEE, 2013, pp. 865–867.
[7] Z. Deng, X. Lin, J. Cai, X. Hu, Battery health estimation with degradation pattern recognition and transfer learning, J. Power Sources 525 (2022), 231027.
[8] Z. Deng, X. Hu, X. Lin, Y. Che, L. Xu, W. Guo, Data-driven state of charge estimation for lithium-ion battery packs based on Gaussian process regression, Energy 205 (2020), 118000.
[9] H. He, X. Zhang, R. Xiong, Y. Xu, H. Guo, Online model-based estimation of state-of-charge and open-circuit voltage of lithium-ion batteries in electric vehicles, Energy 39 (2012) 310–318.
[10] Y. Zhang, W. Song, S. Lin, Z. Feng, A novel model of the initial state of charge estimation for LiFePO4 batteries, J. Power Sources 248 (2014) 1028–1033.
[11] T.-H. Wu, C.-S. Moo, State-of-charge estimation with state-of-health calibration for lithium-ion batteries, Energies 10 (2017) 987.
[12] A. Bartlett, J. Marcicki, S. Onori, G. Rizzoni, X.G. Yang, T. Miller, Electrochemical model-based state of charge and capacity estimation for a composite electrode lithium-ion battery, IEEE Trans. Control Syst. Technol. 24 (2015) 384–399.
[13] S. Skoog, S. David, Parameterization of linear equivalent circuit models over wide temperature and SOC spans for automotive lithium-ion cells using electrochemical impedance spectroscopy, J.Energy Storage 14 (2017) 39–48.
[14] Q. Yu, R. Xiong, C. Lin, W. Shen, J. Deng, Lithium-ion battery parameters and state-of-charge joint estimation based on H-infinity and unscented Kalman filters, IEEE Trans. Veh. Technol. 66 (2017) 8693–8701.
[15] Y. Chen, B. Long, X. Lei, The battery state of charge estimation based weighted least squares support vector machine, in: 2011 Asia-Pacific Power and Energy Engineering Conference, IEEE, 2011, pp. 1–4.
[16] H. Sheng, J. Xiao, Electric vehicle state of charge estimation: nonlinear correlation and fuzzy support vector machine, J. Power Sources 281 (2015) 131–137.
[17] F. Almomani, Prediction the performance of multistage moving bed biological process using artificial neural network (ANN), Sci. Total Environ. 744 (2020), 140854.
[18] F. Almomani, Prediction of biogas production from chemically treated co-digested agricultural waste using artificial neural network, Fuel 280 (2020), 118573.
[19] V.T. Le, E.-N. Dragoi, F. Almomani, Y. Vasseghian, Artificial neural networks for predicting hydrogen production in catalytic dry reforming: a systematic review, Energies 14 (2021) 2894.
[20] M. Shawaqfah, F. Almomani, Forecast of the outbreak of COVID-19 using artificial neural network: case study Qatar, Spain, and Italy, ResultsPhys. 27 (2021), 104484.
[21] F. Yang, S. Zhang, W. Li, Q. Miao, State-of-charge estimation of lithium-ion batteries using LSTM and UKF, Energy 201 (2020), 117664.
[22] S. Tong, J.H. Lacap, J.W. Park, Battery state of charge estimation using a load-classifying neural network, J.Energy Storage 7 (2016) 236–243.
[23] J. Li, M. Liu, State-of-charge estimation of batteries based on open-circuit voltage and time series neural network, in: 2019 6th International Conference on Systems and Informatics (ICSAI), IEEE, 2019, pp. 257–262.

[24] Z. Liu, W. Jia, T. Liu, Y. Chang, J. Li, State of charge estimation of lithium-ion battery based on recurrent neural network, in: 2020 Asia Energy and Electrical Engineering Symposium (AEEES), IEEE, 2020, pp. 742–746.
[25] V.-T. Liu, Y.-K. Sun, H.-Y. Lu, S.-K. Wang, State of charge estimation for lithium-ion battery using recurrent neural network, in: 2018 IEEE International Conference on Advanced Manufacturing (ICAM), IEEE, 2018, pp. 376–379.
[26] S. Hochreiter, J. Schmidhuber, LSTM can solve hard long time lag problems, Adv. Neural Inf. Process. Syst. 9 (1996).
[27] S. Bockrath, A. Rosskopf, S. Koffel, S. Waldhör, K. Srivastava, V.R. Lorentz, State of charge estimation using recurrent neural networks with long short-term memory for lithium-ion batteries, in: IECON 2019–45th Annual Conference of the IEEE Industrial Electronics Society, IEEE, 2019, pp. 2507–2511.
[28] F. Yang, X. Song, F. Xu, K.-L. Tsui, State-of-charge estimation of lithium-ion batteries via long short-term memory network, IEEE Access 7 (2019) 53792–53799.
[29] T. Mamo, F.-K. Wang, Long short-term memory with attention mechanism for state of charge estimation of lithium-ion batteries, IEEE Access 8 (2020) 94140–94151.
[30] X. Shu, G. Li, Y. Zhang, S. Shen, Z. Chen, Y. Liu, Stage of charge estimation of lithium-ion battery packs based on improved cubature Kalman filter with long short-term memory model, IEEE Trans.Transp.Electrificat. 7 (2021) 1271–1284.
[31] X. Chen, K. Hirota, Y. Dai, Z. Jia, Estimation of SOC based on LSTM-RNN and design of intelligent equalization charging system, J.Adv.Comput.Intell.Intell. Informa. 24 (2020) 855–863.
[32] K.L. Wong, M. Bosello, R. Tse, C. Falcomer, C. Rossi, G. Pau, Li-ion batteries state-of-charge estimation using deep LSTM at various battery specifications and discharge cycles, in: Proceedings of the Conference on Information Technology for Social Good, 2021, pp. 85–90.
[33] J. Park, J. Lee, S. Kim, I. Lee, Real-time state of charge estimation for each cell of lithium battery pack using neural networks, Appl. Sci. 10 (2020) 8644.
[34] Z. Wang, A. Fotouhi, D.J. Auger, State of charge estimation in lithium-sulfur cells using lstm recurrent neural networks, in: 2020 European Control Conference (ECC), IEEE, 2020, pp. 1079–1085.
[35] D.P. Kingma, J. Ba, Adam: A method for stochastic optimization. arXiv preprint arXiv:14126980, 2014.
[36] M.H. Sazli, A brief review of feed-forward neural networks, in: Communications Faculty of Sciences University of Ankara Series A2-A3 Physical Sciences and Engineering 50, 2006.
[37] R. Asadi, S.A. Kareem, Review of feed forward neural network classification preprocessing techniques, in: AIP Conference Proceedings, American Institute ofPhysics, 2014, pp. 567–573.